

# Finite Element Analysis for Non-proportional loading

NIMALI T. MEDAGEDARA<sup>1</sup> PDSH GUNAWARDANE<sup>2</sup>

<sup>1,2</sup> Department of Mechanical Engineering,  
Open University of Sri Lanka,  
Nawala, Nugegoda, Sri Lanka.  
[tmmed@ou.ac.lk](mailto:tmmed@ou.ac.lk), [pdgun@ou.ac.lk](mailto:pdgun@ou.ac.lk)

*Abstract:*-Structural components with complex geometries are frequently subjected to alternating loads, which produce multi-axial stresses. In most cases, the loading is non-proportional. Alternating loads tend to initiate fatigue cracks at notches and at other regions of high stresses. Some typical situations in which fatigue can occur are the repeated expansions and contractions of a pressurised aircraft, a car suspension unit absorbing the undulations of a normal road surface and the rhythmic crashing of waves against hull of a ship. However, occurrence of fatigue is a common phenomenon in many engineering components and their failures are also attributed to fatigue.

Knowledge of cyclic deformation behaviour is essential for fatigue analysis of industrial components. However, such knowledge is difficult to obtain for non-proportional loading situations. Although notch deformation can be analysed by methods such as Neuber, these methods are not suitable for critical non-proportional loading paths encountered in industrial components. The aim of this paper is to present cyclic deformation curves for multi-axial varying non-proportional loadings obtained from finite element analysis. The material used was medium carbon steel. It is essential to find the plastic strain ranges under cyclic loads as it is used for fatigue life prediction under variable amplitude tension-torsion multi-axial, non-proportional loops. Hysteresis loops were obtained using ABAQUS Code for different loading conditions of non-proportional loads and the shapes of the loops are discussed for different non-proportional loading paths.

Considering the results obtained from different non-proportional multi-axial loading paths, most damaging and the least damaging non-proportional loading paths have been found.

*Key Words:*- *Finite Element, Non proportional loading, multi axial fatigue*

## 1 Introduction

Many engineering components are subjected to loads with varying amplitude, which vary either proportionally or non-proportionally. Therefore accurate fatigue life assessment is an essential requirement in the life prediction of such design components [1]. Knowledge of cyclic deformation is essential to find the plastic strain ranges, which is used for fatigue life prediction.

The overall aim of this paper is to present the cyclic deformation that is essential to find the plastic strain ranges, which are used for fatigue life prediction under variable amplitude tension-torsion, multi-axial proportional and non-proportional paths. The hysteresis loops were obtained for different load sets of proportional and non-proportional loads and the experimental notch root strains were compared with Finite Element

Analysis (FEA) data obtained using ABAQUS code. The shapes of the hysteresis loops (axial and torsional) also were compared for different proportional and non-proportional loading paths.

## 2 Advantages of using FEA

There are several advantages of using FEA. By using this method complex, two and three-dimensional solids may be represented with reasonable accuracy due to the flexibility of the size and shape of the elements and also bodies incorporating holes and corners may be modelled with ease. The size of the elements incorporated in a domain may vary; thus from FEA it may be refined at critical locations. FEA accuracy is comparable and often better than solutions achieved by means of other analytical or experimental methods. The application of

computer technology to the FEA has led to the general achieve of rapid results [2].

However, it is observed that primary disadvantage of the FEA approach is the need for computer resources associated with vast amount of memory and the computational costs that ensue.

### 3 FE modelling of the notch specimen

The notch specimen used is shown in Fig. 1. The diameter at the notch was selected as 15 mm and the other dimensions were selected to suit the machine requirements.

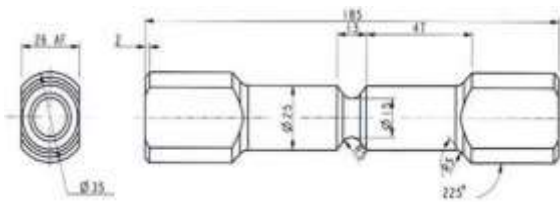
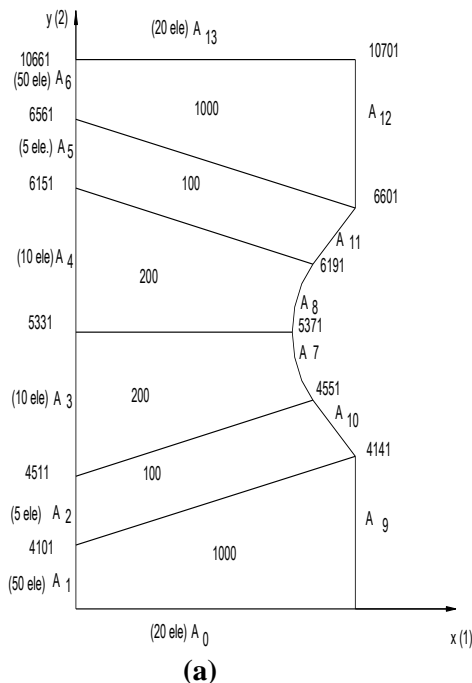


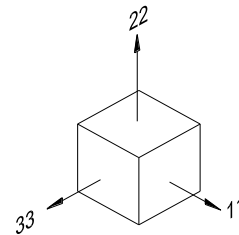
Fig. 1: Dimensions of the specimen

From Peterson's Handbook [3], stress concentration factor at the notch root  $K_t$  was established as 1.6.

### 4 FEA model geometry



(a)



(b)

Fig. 2: (a) Element details (b) Stress or strain directions

As the specimen was geometrically symmetrical, half of the specimen was modeled using ABAQUS code. Fig. 2 (a) shows the selected element details and Fig. 2 (b) shows the stress or strain directions of a block at the notch root of the model.

The total number of elements used for the model was 2,600 and 600 elements were used to define the mesh in notch area as this is the main concern of the investigation. Fig. 3 shows the element density at the notch region.

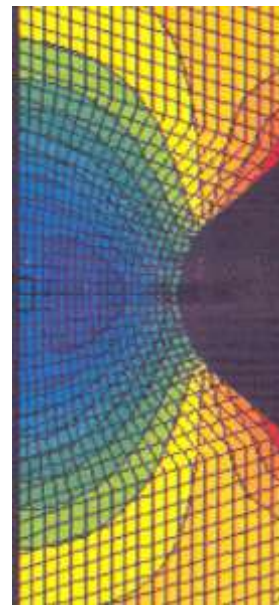


Fig. 3: Element density at the notch

## 5 Details of Meshing

In order to model the specimen, axisymmetric elements with twist (CGAX8 elements) in ABAQUS/Standard is used. This type of element can be used for nonlinear multi-axial loadings. As the specimen is basically a solid circular bar with a notch at the middle of the specimen, these elements could be used. The main aim of the research was to analyse the behaviour of the stress and strain at the notch root. Standard axisymmetric elements could have been used in this case if only the axial loading was considered, but in this study CGAX8 elements (axisymmetric elements with twist) were used because the torsion loading was also considered. This type of element is recommended for studying stress/displacements.

For the CGAX8 elements co-ordinate 1 is radial ( $r$ ) while co-ordinate 2 is axial ( $z$ ). Therefore the  $r$ -direction corresponds to the global  $x$ -direction and  $z$ -direction corresponds to the global  $y$ -direction as shown in Fig. 2 (a). Therefore the degree of freedom 1 is  $U_r$  and the degree of freedom 2 is  $U_z$ . The CGAX8 elements have an additional degree of freedom 5 corresponding to the twist angle  $\phi$  (in radians). The total number of elements used for the model was 2,600. Using 8 noded elements results in a total of 10,661 nodes. Each element has eight nodes as shown in Fig. 4 and each of the nodes have three degrees of freedom.

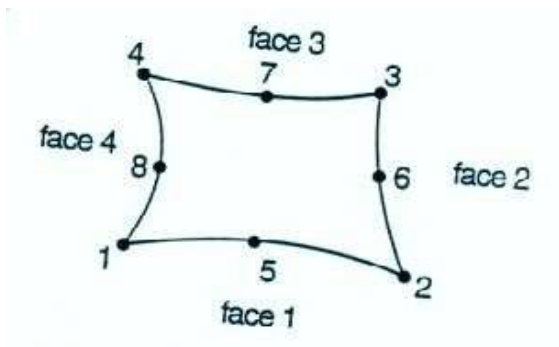


Fig. 4: Node / face numbering of the CGAX 8 element

## 5.1 Loading

As the current research was concerned about the multi-axial loading, the axial load and torque should be applied at the same time. The selected element type was active only for rotational displacement inputs and not for torque input applications.

Therefore when analysing, displacement inputs were used instead of torque. For consistency, both axial and torsion deformations were applied as displacements for every FE analysis.

## 5.2 Constraints

Considering Fig. 2 (a), elements set  $A_0$ , was constrained in axial direction (2 and Z) and transverse direction (5 and twist angle). The elements along the centre line,  $A_1, A_2, A_3, A_4, A_5, A_6$  were constrained in radial direction (1 and X).

## 6.0 Combined axial -torsional loading paths

Cyclic deformation behaviour of the material was investigated under a number of loading paths. In addition to pure axial strain and pure torsion shear strain loadings, two types of combined axial-torsion paths were studied.

- Loading Paths using sinusoidal waveforms
- Loading Paths using non-sinusoidal waveforms

## 6.1 Sinusoidal wave forms

For out-of phase loading, the patterns of the sinusoidal waveforms of shear strain to axial strain are shown in Fig. 5 (a) and the variations of shear strain to axial strain are shown in Fig. 5 (b). For out-of phase loading these variations should be circular or elliptical and the shape will depend on the amplitudes of shear strain, axial strain waveforms and the phase angle.

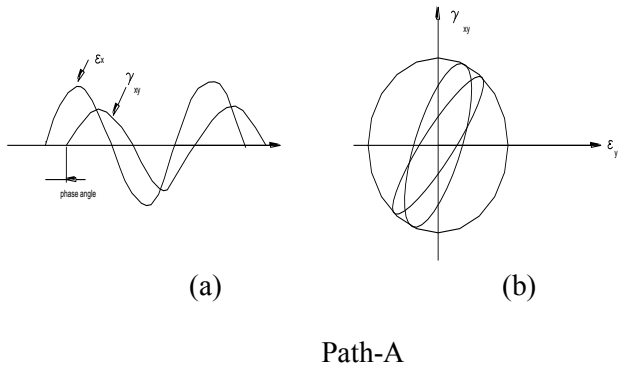


Fig. 5:(a) Waveforms of shear strain to axial strain  
 (b) Variation of shear strain to axial strain for in-phase loading

Phase angle  $\phi$  varies from  $0^0$  to  $90^0$  for both load and torque. Therefore the amplitudes of  $\epsilon_x$  and  $\gamma_{xy}$  were changed to match to the amplitudes of applied load and torque.

### 6.2. Non-sinusoidal waveforms

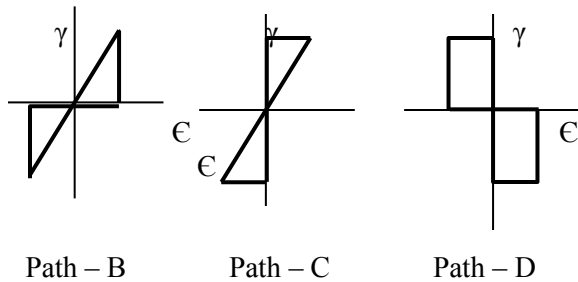


Fig. 6: Non-sinusoidal strain paths

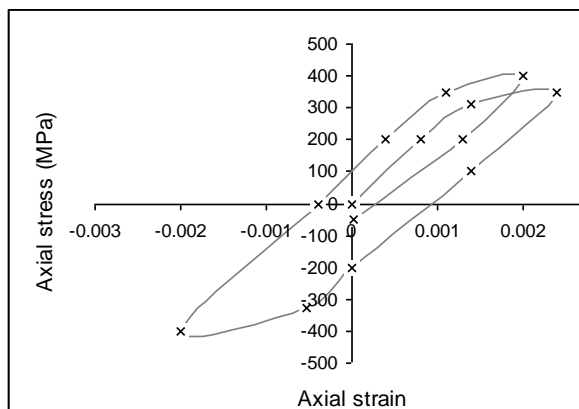


Fig. 7: Graph of axial stress versus axial strain (S22-E22)

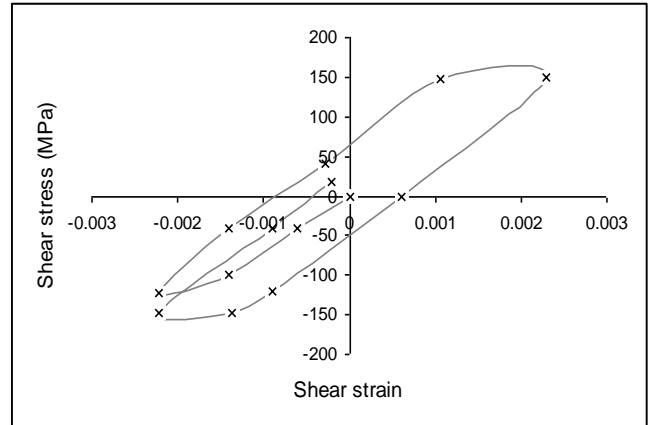


Fig. 8: Graph of shear stress versus shear strain

### 7 Axial and torsional non-proportional loading

When the applied loads cause the directions and the magnitude of the principal stresses and the ratio of the principal stress to change, the loading is termed non-proportional. For the FEA analysis several non-proportional loading Paths were considered and the results are presented in the following sections.

### 8 Non-proportional sinusoidal wave Path-A

As shown in Fig. 9, the specimen was subjected to a  $\pm 0.025$  mm axial displacement (50kN axial load) and  $\pm 0.0025$  rad rotational displacement, (100Nm torque) with  $90^0$  phase difference.

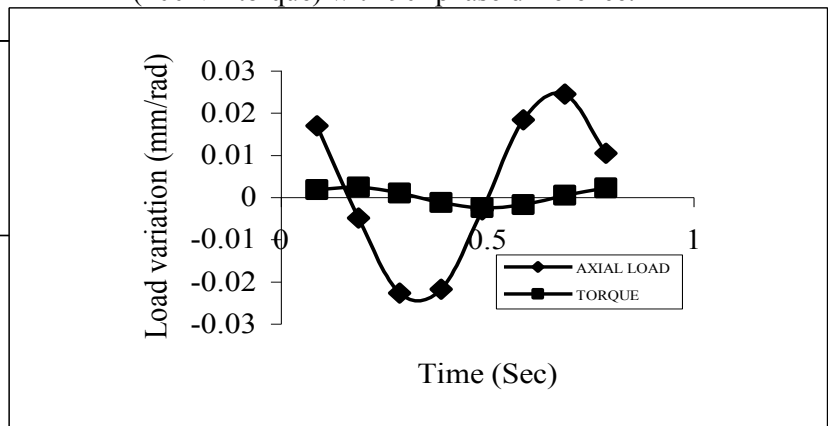
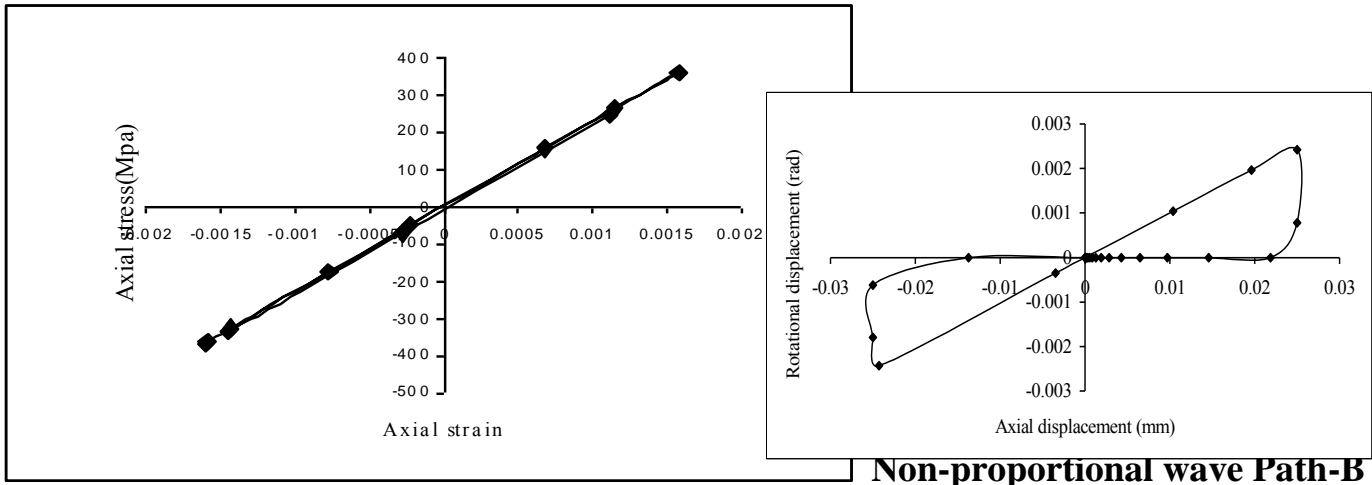


Fig. 9:FEA results - Axial /torque load variation for out of phase loading Path-A



**Non-proportional wave Path-B**

Fig. 10: FEA results - Axial stress versus axial strain at the notch

As shown in Fig. 10, the hysteresis loop shows very little plasticity and the loop is very narrow and long similar to an elastic curve. The gradient of the graph was calculated to be  $2.08E05$  MPa (Elastic Modulus of the material  $E = \sigma / \epsilon$ ).

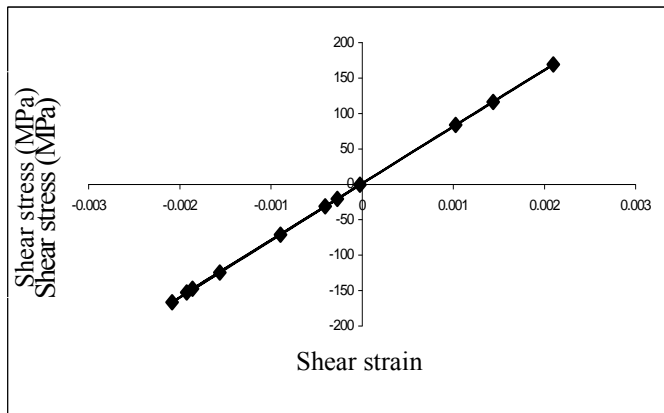
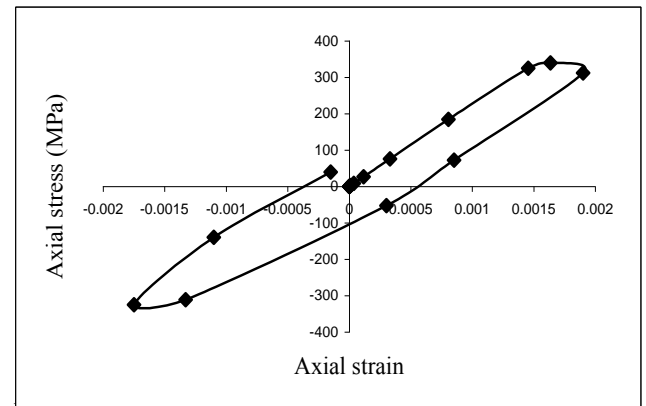


Fig. 11: FEA results - Shear stress versus shear strain (S23-E23) at the notch tip

Fig. 11 shows the elastic behavior and the gradient of the graph was calculated to be  $8.0E07$  MPa. This value is same as the modulus of rigidity of the material.

Fig. 12: Rotational displacement versus axial displacement at the notch root

Fig. 12 shows the applied displacement variations at the notch root. From the ABAQUS code it was difficult to take more convergent values for the non-linear analysis. Therefore the shapes of the loops were little different with expected loops as



shown in Fig. 12. Same behaviour will show for the shear strain versus axial strain at the notch root for the non-proportional loading Path-B

Fig. 13: Axial stress versus strain (S22-E22) at the notch tip for loading Path-B

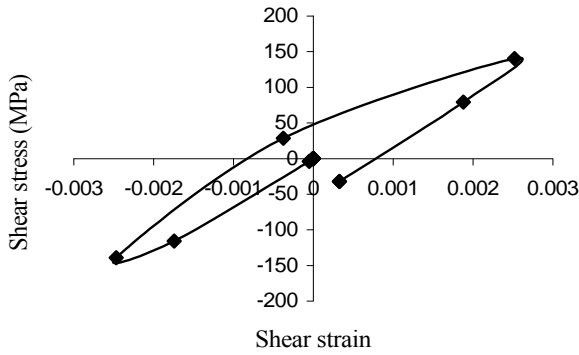


Fig. 14: Shear stress versus shear strain (S23-E23) at the notch tip for loading Path-B

As shown in Figs 13 and 14, both hysteresis loops in Path-B have more energy than the hysteresis loops in Path-A. But there are no noticeable differences between maximum strain values of Paths-A and B.

### 10 Non-proportional wave Path-C

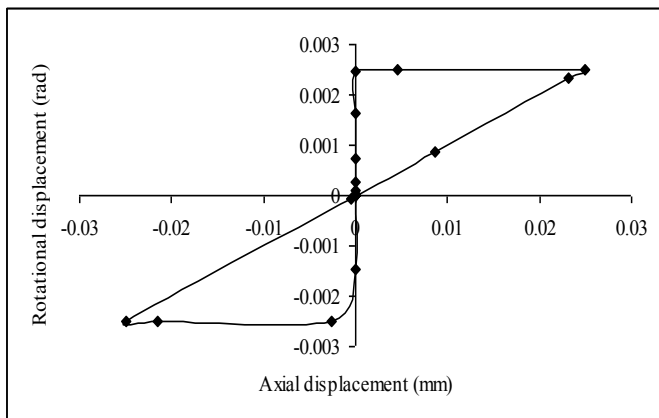


Fig. 15: FEA inputs for non-proportional loading Path-C

Fig. 15 shows the variation of torque versus axial load throughout the wave applied for FEA. The variation is expected to be same for shear strain  $\gamma$  versus axial strain  $\epsilon$  for the loading Path-C.

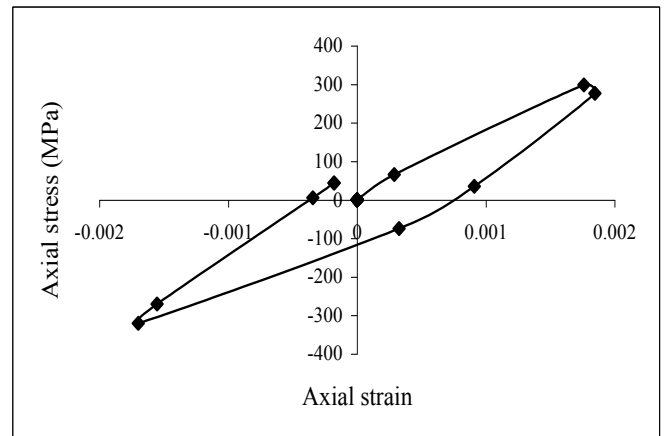


Fig. 16: Axial stress versus axial strain at notch tip for the loading Path-C

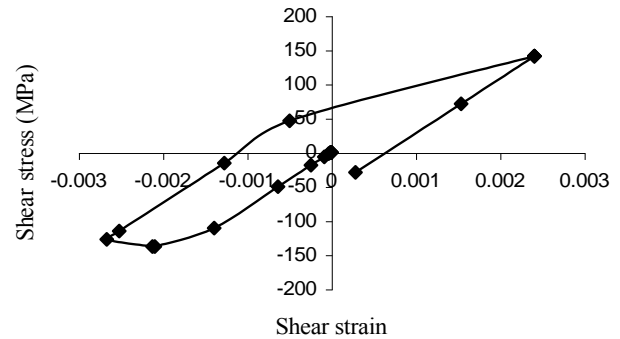


Fig. 17: Shear stress versus Shear strain (S23-E23) at the notch tip for the loading Path-C

Figs 16 and 17 show the axial stress/strain and shear stress/strain loops for loading Path-C. Both loops show plastic energy and during comparison the maximum strain ranges are found to be same for both loops. However, the shapes of the hysteresis loops were different.

### 11 Non-proportional wave Path-D

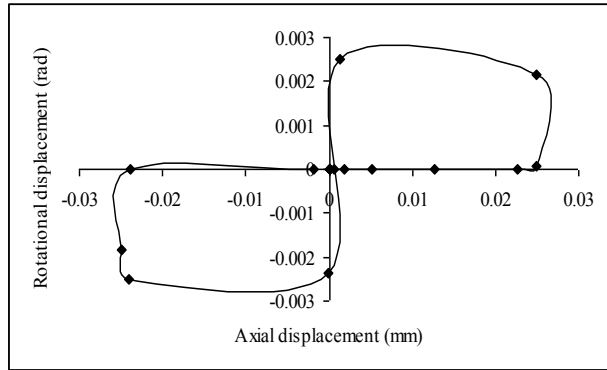


Fig. 18: FEA inputs for non-proportional loading Path-D

Fig. 18 shows the variation of rotational displacement versus axial displacement throughout the wave applied for FEA. As the ABAQUS always does not give many convergent values, the shape of the variation was different as shown in Fig. 18. The variation is expected to be same for shear strain  $\gamma$  versus axial strain  $\epsilon$  for loading Path-D

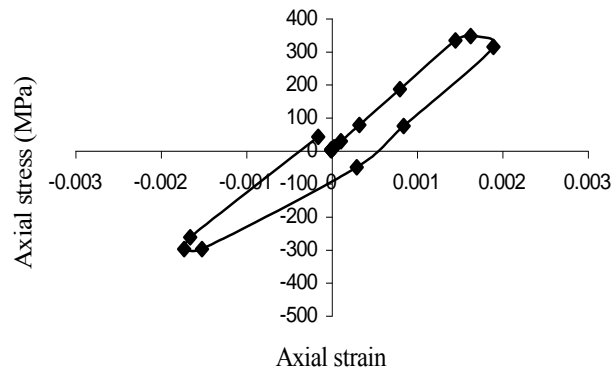


Fig. 19: Axial stress versus axial strain at notch tip for Path - D

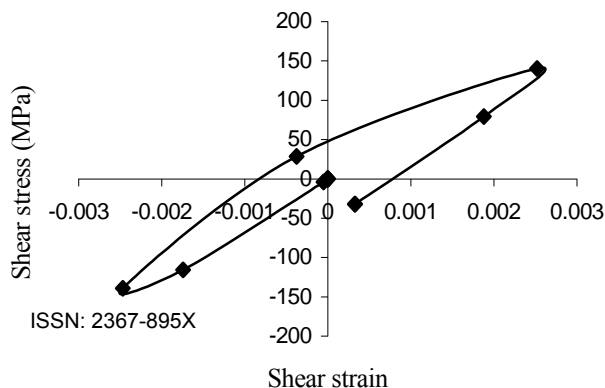


Fig. 20: Shear stress versus shear strain graph for Path-D

Figs 19 and 20 show the hysteresis loops obtained for Path-D non-proportional loading. Both loops show plastic deformation and the shapes of the loops are completely different.

The size of the elements and the type of elastic-plastic theory can influence the results obtained by FEA. Another factor that can influence FEA results is the assumptions made in the numerical solution. However the finite element analyses did show that the stresses and strains are higher at the notch root

### 12 Results

Table 1: The axial and shear strain ranges for each test

Non-proportional Paths	$\Delta\epsilon$	$\Delta\gamma$
Path-A	0.0030	0.0029
Path-B	0.0038	0.0035
Path-C	0.0040	0.0055
Path-D	0.0040	0.0050

### 13 Conclusion

The behavior of hysteresis loops (cyclic deformation) for material (mild carbon steel) under uniaxial, torsion, proportional and different non-proportional loadings was studied using the Finite Element Analysis (ABAQUS code).

The strain-life method is commonly used to predict fatigue crack initiation, and it requires knowledge of notch-root stresses and strains.

These quantities can be determined in several ways such as direct strain gauge measurements, using finite element analysis or by using approximate methods that relate local stresses and strains to their remote values. But for multi-axial loading still there is no universally acceptable method to analyse fatigue life. But for strain-life method, shear and axial strain ranges are more important for the analysis.

FEA results here shown significant difference in hysteresis behaviour under each non-proportional loading. From the observations, it is clear that non-proportional loading Path-C is prone to more damage and loading Path-A is least damaging in terms of fatigue life.

*References:-*

- [1] Andrzej BUCZYNSKI and Grzegorz Glinka, 1997, Elastic-Plastic Stress-Strain Analysis of notches under non-proportional loading, Proceeding of the 5th international conference on Biaxial/Multi-axial Fatigue and Fracture Cracow'97, Poland, pp 461-479.
- [2] Segerlind L.J., 1976, Applied Finite Element Analysis, John Wiley and Sons.
- [3] Peterson R.E, 1974, Stress Concentration factors, New York: Wiley